Mechanics of Advanced Composite Structures 5 (2018) 83–90

Semnan University

Mechanics of Advanced Composite Structures

journal homepage: http://MACS.journals.semnan.ac.ir

Capillary Effects on Surface Enhancement in a Non-Homogeneous Fibrous Porous Medium

M.R. Shahnazari*, M. Esfandiar

Department of Mechanical Engineering, K. N. Toosi University of Technology, Tehran 1999143344, Iran

PAPER INFO

Paper history:
Received 2016-08-20
Revised 2017-06-04
Accepted 2017-08-22

Keywords:
Vacuum-assisted resin transfer molding
Free surface
Capillary pressure
Porous media
Finite element.

ABSTRACT

The evaluation of a free fluid surface in a porous medium has several mathematical applications that are important in industries using molds, particularly in the fluid injection process. The vacuum-assisted resin transfer molding (VARTM) process is a promising technology in the primary composite industry. An accurate computational simulation of the VARTM process would be a cost-effective tool in the manufacturing of composites. In this paper, capillary effects were incorporated into an existing resin transfer molding model to simulate VARTM processing. To increase the accuracy of the VARTM process simulation, the effect of capillary pressure on a surface without flow was studied using the boundary element method. The simulation results were close to the experimental data reported by other researchers. It can be concluded that better reliability and accuracy could be achieved from theoretical predictions by examining the effects of capillary pressure on flow injection into porous materials.

1. Introduction

The problem of surface enhancement in porous media that can be infiltrated by fluids has become an important consideration in many industrial processes. This phenomenon has a significant effect on various applications, such as solidification in casting, crude oil, and extraction. Vafai and Srinivasan [1] analyzed the surface enhancement of a system containing two immiscible materials. Binetruy et al. [2] studied a two-dimensional (2D) flow of a porous medium in a duct using a marker-and-cell (MAC) method. The phenomenological analysis of free surface transport through porous media was investigated by Chen and Vafai [3], and constant porosity is assumed in this analysis. Resin transfer molding (RTM) has become a widely used process to manufacture glass-reinforced composites. A good description of the basic technical issues of RTM manufacturing can be found in a reference book by Cauchois [4]. RTM is a fabrication technique using closed molds that reduces the resin curing time. In this process, stacked, dry fibrous reinforcements are placed in the cavity of a rigid mold, and resin is injected at low pressure. The stiffness of the mold is often a concern during the manufacturing of large parts with a high fiber volume content. Although the filling time can be increased significantly, sometimes it is not possible to inject resin into the part. A higher injection pressure could reduce the injection time, but the cost of the required equipment may be too high for low volume productions.

Another limitation of injection pressure is point void avoidance in composite products. The liquid composite molding (LCM) process variant of vacuum-assisted resin infusion (VARI) was first introduced in the Marco method [4]. It enables large parts to be successfully manufactured at a relatively low cost. In this process, stacked, dry fibrous reinforcements are placed between a stiff mold and a

* Corresponding author. Tel.: +98-21-84063260; Fax: +98-21-88049074
E-mail address: shahnazari@kntu.ac.ir

DOI: 10.22075/MACS.2017.1558.1074

plastic bag. Resin is injected by gravity after a partial or total vacuum is achieved in the cavity containing the reinforcement. Most of the vacuum-driven techniques that are now commonly used in many industrial applications are based on trial-and-error testing.

Williams et al. [5] have reviewed the main developments in infusion composite manufacturing process. From the VARI process developed by Group Lotus Cars Ltd. [6] to Seemann's composite resin infusion molding process (SCRIMP) [7], many variants of resin infusion are now used by various companies. The main advantages of these techniques lie in their tooling cost, which is lower than that of RTM that uses closed molds. An original and optimized approach to resin infusion was developed by Kaizen Technologies under the name of the Kaizen Infusion System (KIS). The behavior of resin during the infusion process is not yet fully understood, and the processing strategy used in many applications is not always optimal [8, 9].

Capillary pressure is defined as the energy per unit volume of a porous medium needed for replacing a gas (or vacuum) with a liquid. Capillary effects have been shown to be a determinant in the mechanisms of void formation for the infiltration of fabrics [2, 10]. There is an optimal infiltration velocity that produces composites with minimal void content. Below that velocity, capillary forces dominate, and the infiltration process leads to void formation in the inter-tow region. But above the optimal value, viscous flow dominates, and voids are mainly created within the fiber tows [11].

Several studies have been conducted to determine the magnitude of capillary pressure developed in synthetic fabric infiltration. Batch et al. [12] investigated the capillary impregnation of aligned fibrous beds and found an optimal fluid speed at which micro and macro fluid speed with minimized void formation.

Patel and Lee [10] analyzed resin-fiber wettability by conducting a wicking test and measuring capillary pressure using different test fluids. As a general trend, they found an increase in capillary pressure with a decrease in matrix-fiber surface tension. Capillary pressures obtained for dioctyl phthalate (DOP) fluid and glass fiber (40–60 vol%) were in the order of 10 kPa. Following the same experimental approach, Amico and Lekakou [13, 14] conducted capillary rise experiments on glass fiber bundles with epoxy resin and silicon oil. They found a good correlation between the experimental and theoretical values of equilibrium capillary pressure for epoxy resin (9.6 KPa). Nevertheless, they did not explore the dynamic effects of capillary pressure. Verrey et al. [15] conducted infiltration experiments on non-crimp fabrics with different test fluids. They found negative values of capillary pressure for polyethylene glycol and lauryllactam 12 and positive values for an epoxy resin. However, in the last case, they found that for low numbers of capillaries (low fluid velocity), the resin changed its behavior from non-wetting to wetting, resulting in flows enhanced by capillary forces. A number of studies have been devoted to the experimental methods dedicated to measuring static and dynamic contact angles between single fibers and liquid, on both synthetic [16-20] and natural fibers [21-25].

Using a flow analysis network (FAN) method, Stoll et al. [26] have simulated the RTM process. The results were presented as mold filling time and free fluid surface state based on time. Acheson et al. [9] presented a 2D simulation for mold filling. The capillary effect has an important role in simulating processes with a low flow rate or low pressure injection, such as the VARTM process. The capillary effect during LCM with natural fibers has been investigated by Francucci et al. [27]. Setaguchi et al. [28] have focused on the wetting process in a glass fiber–resin system. They illustrated changes in wetting behavior by comparing the flow rate at the resin tip with that in the resin bulk.

Numerical simulation of resin injection can assist in positioning the inlet ports and vacuum intakes, especially for large and complex parts. Optimal injection strategies can be studied on a virtual model prior to prototype testing, consequently helping to reduce process set-up costs.

The goal of this investigation is to verify the VARTM process with sufficiently accurate simulations of resin infusion, which can be performed using numerical tools that were originally developed for classical RTM, that is, to simulate the injection of resin in rigid molds. In this paper, the simulation of a VARTM process for a non-homogeneous porous medium has been studied. The verified parameters included flow front patterns and infiltration times. To increase the accuracy of the presented simulation, the effect of capillary pressure on a surface without flow has been studied. Using the boundary element method (BEM), the fluid flow with or without capillary effects was analyzed, and the numerical results were compared with the results of other studies. By comparing the results obtained from two cases with other results, it was found that the results can be improved by paying attention to the capillary effects.

2. Theory

The flow of resin throughout the reinforcement process is well described by Darcy's law, which predicts a linear relation between the local flux density and the applied pressure gradient. Darcy's law is generalized to three dimensions, and the continuity equations are as follows:

$$u = \frac{K}{\mu}\left(\nabla P - \rho_f g\right) \tag{1}$$

$$\nabla \cdot u = \circ , \tag{2}$$

where u is the local flux density (or superficial velocity), K is the permeability tensor, μ is the resin viscosity, P is the pressure of the resin, ρ_f is the (local) resin density, and g is the gravity vector [29]. The substitution of Darcy's law (Eq. 1) in Eq. 2 results in a formulation of the continuity equation, where the only unknown parameter is pressure (a three-dimensional [3D] scalar quantity) within the fluid in the mold:

$$\nabla \cdot \left[\frac{K}{\mu}\left(\nabla P - \rho_f g\right) \right] = \circ \tag{3}$$

The permeability of a preform depends on several factors, the main one being its porosity. Several analytical models have been proposed to predict the permeability of a fibrous reinforcement [30]. Usually, experimental measurements are required to obtain the value of this key parameter. The most commonly used empirical model to describe the permeability of fiber porosity is as power low function. Therefore, by considering a non-homogenous porous medium, the constant permeability can be shown in terms of porosity values, as follows:

$$K = A \cdot \varepsilon^{B} , \tag{4}$$

where A and B can be estimated by experimental measurements [31]. Also, the porous media porosity, ε, can be determined by

$$\varepsilon = 1 - \frac{A_s}{\rho_p t_p} , \tag{5}$$

where A_s is the areal weight or superficial density, ρ_p is the density, and t_p is the thickness of the preform. The areal weight was determined by measuring the weight of the preform, which was divided by the area to yield units of grams per square meter. The density of the preform was assumed to be equal to the density of the fiber itself, which was provided by the manufacturer [31].

In a 50-kPa vacuum, the fiber porosity was $\varepsilon = 51\%$. Based on the experiments of Loos and Sayre [29], we assumed that the equivalent permeabilities were 5.26 E–11m^2 and 8.73 E–11 m^2 for 2.97 mm and 5.94 mm thicknesses, respectively.

3. Numerical Solution

The mathematical models for filling an LCM mold were solved with a set of partial differential equations. The finite element formulation was based on the procedure outlined by Reddy [32] and expressed for an element as

$$[K_{ij}^{n}][P_j^{n} - \rho g_j^{n}] = [F_i^{n}] , \tag{6}$$

where K_{ij}^{n} and F_i^{n} are as follows:

$$K_{ij}^{n} = \int_{\Omega_n} \frac{K_{ij}}{\mu} N_{\alpha,i} N_{\beta,j} d\Omega \tag{7}$$

$$F_i^{n} = \int_{\Gamma_n} Q N_{\alpha} d\Gamma + \int_{\Omega_n} \frac{K_{ij}}{\mu} \rho g_j N_{\alpha,i} d\Omega \tag{8}$$

In Eqs. (6), (7) and (8), Ω_n is the domain of an element, Γ_n is the surface of an element, P_j^{n} is the pressure at each node, ρg_j^{n} is the pressure due to gravity at each node, Q is the specified flux through the face of an element, and N is a linear interpolation function [29].

The process simulation model was used to investigate the resin infiltration of a 60.96-cm-by-30.48-cm preform during the VARTM process. The media was subdivided into a finite number of tetrahedrons, triangles (a 2D shell element with constant thickness), and runners (a one-dimensional [1D] line element with a constant cross-section of an arbitrary shape). Figs. 1 and 2 show the finite element meshes of E-glass performance models for 2.97-mm and 5.94-mm thicknesses, respectively. The mesh of the E-glass preforms consisted of 3,642 and 5,376 elements, respectively.

Mesh independence was checked for the proposed model by measuring relative errors in the numerical results of the predicted infiltration time values. The computational mesh of the 2.97-mm E-glass preform with 3,642 elements showed less than 4% difference with a finer mesh with 4,124 elements and was accepted. Similarly, mesh independency was evaluated for the 5.94-mm E-glass preform model, and a relative error of less than 5% was achieved. A computational mesh with 5,376 elements was accepted after it was compared with a finer mesh with 5,921 elements.

An approximation was calculated for the pressure as a linear combination of basic functions N:

$$\tilde{P}(t) = \sum P_j(t) N_j \, , \tag{9}$$

where P is the pressure and N is a linear interpolation function [33].

The position of the flow front was tracked by assigning filling factors to the nodes. Initially, all nodes were empty (f = 0), except for the injection nodes. Here, pressure was calculated in fully filled nodes (f = 1). All partly filled nodes (0 < f < 1) resulted in the formation of pressure at the flow front, which was set to zero in all nodes that were not already filled (i.e., empty and front nodes).

The main boundary conditions for solving equations (6) include

- A flow front pressure condition: $2\gamma_{lv}\cos\theta / r_h$
- A constant pressure condition at the inlet: $P_{\text{inlet}} = P$
- A velocity normal to the boundary wall of zero: $V \cdot \vec{n} = 0$,

where $\vec{n}$ is the vector normal to the boundary, γ_{lv} is the surface tension, θ is the contact angle, and r_h is the hydraulic radius of the fiber bundle, defined as the cross-sectional area normal to the flow divided by the perimeter applied to the fluid.

If the geometry of a unidirectional fiber bundle is considered, r_h can be defined based on two flow directions: parallel to and perpendicular to the fiber. In this research, a case in which the flow is perpendicular to a unidirectional fiber bundle was chosen. This was because the impregnation of the 1,523 E-glass preforms used in the capillary pressure modeling occurred primarily in a transverse direction. Thus, for a flow perpendicular to a unidirectional fiber bundle, r_h was determined to be

$$r_h = \frac{d_p}{2}\left(\frac{\varepsilon}{1-\varepsilon}\right), \tag{10}$$

where d_p is the characteristic particle diameter of the 1,523 E-glass fiber and is equal to 18 E-6 m [29].

In this research, a constant capillary pressure was assumed using a static contact angle. In reality, this contact angle could increase in value as the viscous drag becomes significant, which would reduce the capillary pressure. Therefore, the capillary pressure generated during processing may be smaller than the values theoretically calculated here.

4. Results and Discussion

In molding processes, the evaluation of a free surface is an important factor in fluid injection modeling. Fig. 3 shows the free surface position in Z-direction with a comparison of the results obtained by Vafai and Srinivasan [1] for a 1D flow front pattern. The capillary pressure was modeled using a boundary condition modification and was evaluated using the fiber porosity, surface tension, and contact angle values for the E-glass–resin system.

In Fig. 3, X_0 denotes the location of the interface, L is the horizontal extent of the preform, and Re_k denotes the Reynolds number, defined by permeability as $Re_k = \rho\sqrt{K}u/\mu$. The model of RTM flow was first verified without the influence of capillary pressure. In this verification, two important factors were examined.

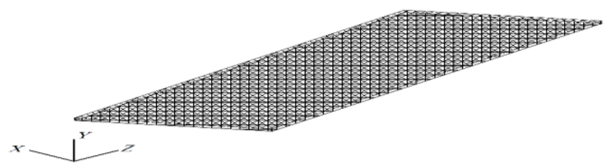

Figure 1. Finite element mesh of a 2.97-mm 1,523 E-glass preform

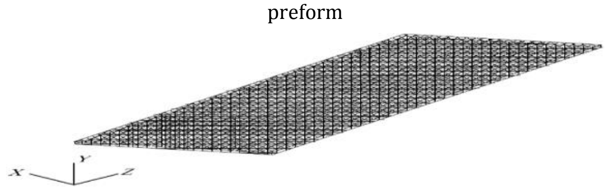

Figure 2. Finite element mesh of a 5.94-mm 1,523 E-glass preform

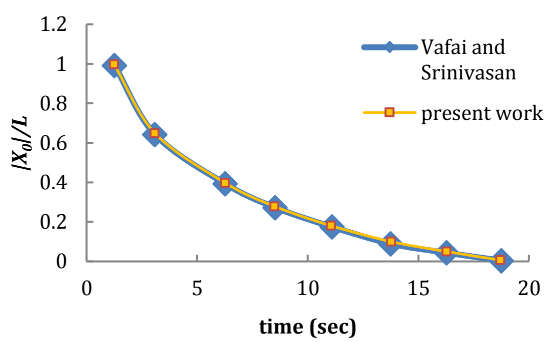

Re_k=5*10^{-10}, K=10^{-10}

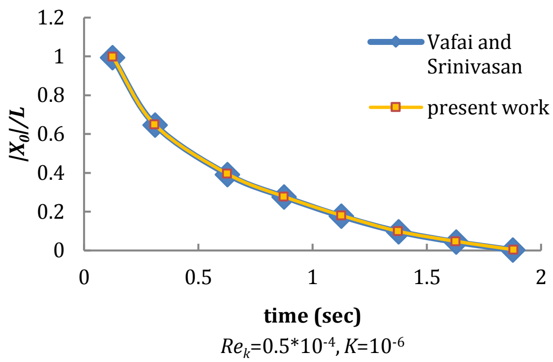

Figure 3. Free surface position in comparison with the results obtained by Vafai and Srinivasan [1]

The first was the flow front pattern. It was desirable to have an accurate simulation of the flow front patterns during processing to determine the placement of resin–vacuum ports and to examine possible areas where void formation could occur. The second factor was the infiltration time, which was necessary for one obvious reason: Without a verification of the simulated infiltration time, an accurate prediction of the experimental processing time would not be available.

The flow front patterns during the VARTM process were verified by comparing the modeled and observed flow patterns during the infiltration of 2.97-mm and 5.94-mm E-glass preforms. Figs. 4 and 5 show the flow front pattern for E-glass preforms without considering capillary pressure, and these patterns are based on infiltration time.

Figs. 6 and 7 show the influence of capillary pressure on the flow front pattern and the infiltration time for the 2.97-mm and 5.94-mm E-glass preforms, respectively. From these patters, it can be stated that by considering capillary pressure effects, the infiltration times for two models have been reduced. Capillary effects are one of the most important causes of this reduction in infiltration time. Therefore, considering the capillary effects on the VARTM process, which is a method for manufacturing complex structures with various fiber laminates, is crucial. Misusing a proper runner distribution system in the infiltration process may cause a decrease in the vacuum pressure applied to the preform. However, the decrease in vacuum pressure leads to an increase in resin velocity. Slower injection speeds favor better bonding and wetting. Consequently, fingering appears at the flow front as a result of differing permeability. Fingering depends on the fluid rate, and the number of capillaries could easily show this dependency.

The effect of capillary pressure is necessary because the low pressure used for infiltration (~1 atm) produced small pressure gradients throughout the preform. Therefore, a lack of attention to capillary effects leads to these events and, finally, causes dry spot formation. Dry spots are a common void formation where a dry area results because of the inability of the resin to infiltrate a particular region of the preform. The strength and surface quality of parts manufactured by the VARTM process depends on void formation. Therefore, considering capillary effects could prevent undesirable construction defects in the manufacturing process.

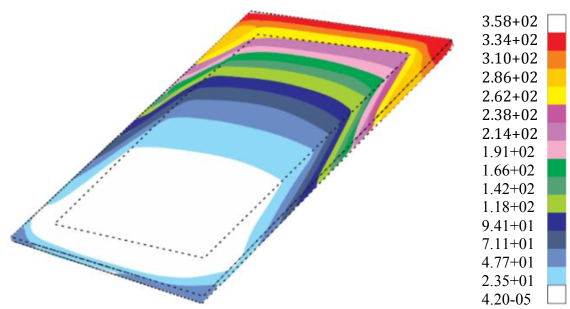

Figure 4. Flow front pattern for a 2.97-mm E-glass preform without considering capillary pressure

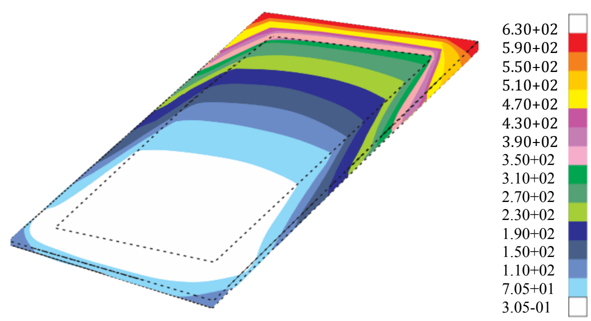

Figure 5. Flow front pattern for a 5.94-mm E-glass preform without considering capillary pressure

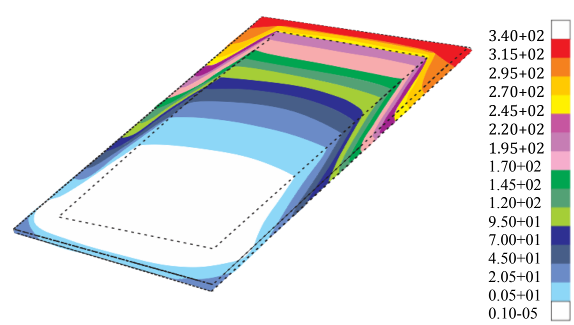

Figure 6. Flow front pattern for a 2.97-mm E-glass preform with capillary pressure consideration

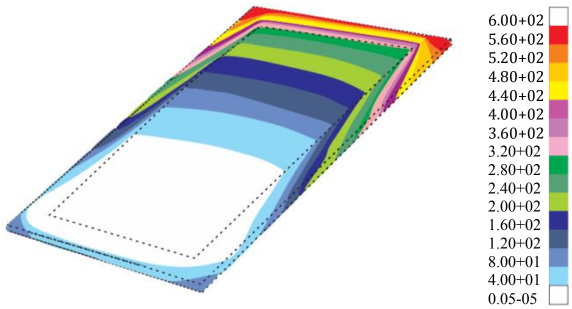

Figure 7. Flow front pattern for a 5.94-mm E-glass preform with capillary pressure consideration

Infiltration times give a much more quantitative measure for model verification than flow front pattern observations do. Table 1 shows the infiltration time for the E-glass–resin system in this study. In the table, the measured time by Stoll et al. [26] is compared with the results of the numerical solution in two cases, with and without considering capillary pressure. This table also presents the experimental results achieved by Stoll et al. [26] and Loos and Sayre [29]. These results show that the calculated infiltration time could be improved by considering capillary pressure effects. It is clear from Table 1 that the values from the numerical results that consider capillary pressure are much closer to the experimental results.

Table 2 presents the relative errors of the data introduced in Table 1. To determine the effects of capillary pressure, a comparison is made between experimental results (obtained by Stoll et al. [26] and Loos and Sayre [29]) and numerical results that consider capillary pressure. Numerical results without the capillary pressure consideration are also compared with the numerical results presented by Stoll et al. [26].

When capillary pressure is neglected, simulated infiltration times for both the 2.97-mm and 5.94-mm E-glass preforms were over the predicted experimental times by 8–9%. By considering the effects of capillary pressure on infiltration time for the 2.97-mm E-glass preform, it can be seen from Table 2 that the model calculated infiltration time is now within 2% of the infiltration times of 332 seconds obtained by Stoll et al. and 330 seconds obtained by Loos and Sayre. When capillary pressure is considered for the 5.94-mm E-glass preform, the simulated infiltration time is within 3% of the time of 585 seconds measured by Loos and Sayre, and it is within 0.7% of the time of 606 seconds measured by Stoll et al. According to the relative error values, it can be observed that there is an acceptable compatibility with other results.

Table 1. Infiltration time for an E-glass–resin system

Fiber thickness (mm)	Experimental results		Numerical results		
			Without capillary pressure		With capillary pressure
	Stoll et al. [26]	Loos and Sayre	Stoll et al. [26]	Present work	Present work
2.97	332	330	357	358	338
5.94	606	585	629	638	602

Table 2. Relative error of infiltration time results

Fiber thickness (mm)		2.97	5.94
Numerical results without capillary pressure	Stoll et al. [26]		
	Present work	1.8%	0.7%
Experimental results	Stoll et al. [26]		
Numerical results with capillary pressure	Present work	0.3%	1.4%
		2.4%	2.9%
Experimental results	Loos and Sayre [29]		

5. Conclusion

A simple approach to simulate resin infusion was presented. Models with and without capillary pressure were simulated of plug flows in the in-plane direction. It can be seen from the results that the calculated infiltration time in capillary pressure consideration was within 2–3% of the measured infiltration time, in contrast to the 8–9% margin when capillary pressure was neglected. Based on these results, it is postulated that capillary pressure plays an important role in VARTM processing. Further modeling of capillary pressure can provide significant insight into this phenomenon. In this research effort, a constant capillary pressure was assumed using a static contact angle. In practice, this contact angle could increase in value as the viscous drag becomes significant, which would reduce the capillary pressure. Therefore, the capillary pressure generated during processing may be smaller than the values theoretically calculated here. Although the later statement may be true, these results show the capability of capillary pressure to reduce simulated infiltration times as much as 6% for the low pressure injection process.

Nomenclature

u	Superficial velocity
K	Permeability
μ	Viscosity
P	Pressure
ρ_f	(Local) resin density
g	Gravity vector
A, B	Experimental coefficients in Eq. 4
ε	Porosity
A_s	Areal weight or superficial density of the preform
ρ_p	Density of the preform
t_p	Thickness of the preform
Ω_n	Element domain
Γ_n	Element surface
P_j^n	Pressure at each node
ρg_j^n	Pressure due to gravity at each node
Q	Specified flux through the face of an element
N	Linear interpolation function (shape function)
$\vec{n}$	Normal vector
γ_{lv}	Surface tension
θ	Contact angle
r_h	Hydraulic radius
d_p	Characteristic particle diameter of fiber
X_0	Location of the interface
L	Horizontal extent of the preform
Re_k	Reynolds number defined by permeability

References

[1] Srinivasan V, Vafai K. Analysis of linear encroachment in two-immiscible fluid systems in a porous medium. *Journal of fluids engineering*. 1994; 116:135-9.

[2] Binetruy C, Pabiot J, Hilaire B. The influence of fiber wetting in resin transfer molding: scale effects. Polymer composites. 2000; 21:548-57.

[3] Chen S, Vafai K. Analysis of free surface momentum and energy transport in porous media. *Numerical Heat Transfer, Part A: Applications*. 1996; 29:281-96.

[4] Cauchois J. R.T.M. Process. Editions Syntech. 1997; 228: Marco Method, US Patent No. 2495640(1950).

[5] Williams C, Summerscales J, Grove S. Resin infusion under flexible tooling (RIFT): a review. *Composites Part A: Applied Science and Manufacturing*. 1996; 27:517-24.

[6] Group Lotus car Ltd. Vacuum Molding Patent, Gb Patent No. 1432333. 1972.

[7] Seemann III WH. Plastic transfer molding techniques for the production of fiber reinforced plastic structures. US Patent No. 5,052,906; 1990.

[8] Chittajallu KM. Computational modeling of the vacuum assisted resin transfer molding (VARTM) process: Clemson University; 2004.

[9] Acheson JA, Simacek P, Advani SG. The implications of fiber compaction and saturation on fully coupled VARTM simulation. *Composites Part A: Applied Science and Manufacturing*. 2004; 35:159-69.

[10] Patel N, Lee LJ. Modeling of void formation and removal in liquid composite molding. Part I: Wettability analysis. *Polymer composites*. 1996; 17:96-103.

[11] Ruiz E, Achim V, Soukane S, Trochu F, Bréard J. Jute Fibers Under Scanning Electron Microscopy. *Composites Science and Technology*. 2006; 66:475.

[12] Batch GL, Chen Y-T, Macoskot CW. Capillary impregnation of aligned fibrous beds: experiments and model. *Journal of reinforced plastics and composites*. 1996; 15:1027-51.

[13] Amico S, Lekakou C. Axial impregnation of a fiber bundle. Part 1: capillary experiments. *Polymer composites*. 2002; 23:249.

[14] Amico S, Lekakou C. Axial impregnation of a fiber bundle. Part 2: theoretical analysis. *Polymer composites*. 2002; 23:264-73.

[15] Verrey J, Michaud V, Månson J-A. Dynamic capillary effects in liquid composite moulding with non-crimp fabrics. *Composites Part A: Applied Science and Manufacturing*. 2006; 37:92-102.

[16] Miller B, Penn LS, Hedvat S. Wetting force measurements on single fibers. *Colloids and Surfaces*. 1983; 6:49-61.

[17] Lu W, Fu X, Chung D. A comparative study of the wettability of steel, carbon, and polyethylene fibers by water. *Cement and concrete research*. 1998; 28:783-6.

[18] Park J-M, Kim D-S, Kong J-W, Kim M, Kim W, Park I-S. Interfacial adhesion and micro-failure modes of electrodeposited carbon fiber/epoxy–PEI composites by micro-droplet and surface wettability tests. *Journal of colloid and interface science*. 2002; 249:62-77.

[19] Xu Z, Chen L, Huang Y, Li J, Wu X, Li X, et al. Wettability of carbon fibers modified by acrylic acid and interface properties of carbon fiber/epoxy. *European polymer journal*. 2008; 44:494-503.

[20] Song W, Gu A, Liang G, Yuan L. Effect of the surface roughness on interfacial properties of carbon fibers reinforced epoxy resin composites. *Applied surface science*. 2011; 257:4069-74.

[21] Krueger JJ, Hodgson KT. Single-fiber wettability of highly sized pulp fibers. *TAPPI journal*. 1994.

[22] Pietak A, Korte S, Tan E, Downard A, Staiger MP. Atomic force microscopy characterization of the surface wettability of natural fibres. *Applied surface science*. 2007; 253:3627-35.

[23] Fuentes C, Tran LQN, Dupont-Gillain C, Vanderlinden W, De Feyter S, Van Vuure A, et al. Wetting behaviour and surface properties of technical bamboo fibers. *Colloids and Surfaces A: Physicochemical and Engineering Aspects*. 2011; 380:89-99.

[24] Tran LQN, Fuentes C, Dupont-Gillain C, Van Vuure A, Verpoest I. Wetting analysis and surface characterisation of coir fibres used as reinforcement for composites. *Colloids and Surfaces A: Physicochemical and Engineering Aspects*. 2011; 377:251-60.

[25] Fuentes C, Tran LQN, Van Hellemont M, Janssens V, Dupont-Gillain C, Van Vuure A, et al. Effect of physical adhesion on mechanical behaviour of bamboo fibre reinforced thermoplastic composites. *Colloids and Surfaces A: Physicochemical and Engineering Aspects*. 2013; 418:7-15.

[26] Stoll F, Banerjee R, Campbell S, Day S. Manufacture of fiber-reinforced-foam composite sandwich structures. Sixteenth Technical Conference of the American Society for Composites2001. p. 2001.

[27] Francucci G, Vasquez A, Rodriguez S, Ruiz E. Capillary Effect in Assisted Resin Transfer Modeling with Natural Fibers Proceedings of The 10th Int Conference on Flow Process in Composite Material, (FPCM). Monte Verita, Ascuna CtlJuly 2010. p. 11-5.

[28] Setaguchi T, Fukahara Y, Veno L, Ogihara S, Watanabe K. Wetting Behaviors in Resinf- Fiber System. Proceedings of the 8th Int Conference on Composite Materials. Jeju Island, Korea2011.

[29] Loos AC, Sayre J. RFI and SCRIMP Model Development and Verification. 2000.

[30] Dullien FA. Porous media: fluid transport and pore structure: Academic press; 2012.

[31] Joubaud L, Achim V, Trochu F. Numerical simulation of resin infusion and reinforcement consolidation under flexible cover. *Polymer composites*. 2005; 26:417-27.

[32] Reddy JN. An introduction to the finite element method: McGraw-Hill New York; 1993.

[33] Petrolito J. Approximate solutions of differential equations using Galerkin's method and weighted residuals. *International Journal of Mechanical Engineering Education*. 2000; 28:14-26